

# *Impact of granular behaviour of fragmented sea ice on marginal ice zone dynamics*

Conference or Workshop Item

Accepted Version

Rynders, S., Aksenov, Y., Feltham, D. L. ORCID: <https://orcid.org/0000-0003-2289-014X>, Nurser, A. J. G. and Madec, G. (2022) Impact of granular behaviour of fragmented sea ice on marginal ice zone dynamics. In: IUTAM Symposium on Physics and Mechanics of Sea Ice, 3-9 Jun 2019, Aalto University, Espoo, Finland. doi: [https://doi.org/10.1007/978-3-030-80439-8\\_13](https://doi.org/10.1007/978-3-030-80439-8_13) Available at <https://centaur.reading.ac.uk/102511/>

It is advisable to refer to the publisher's version if you intend to cite from the work. See [Guidance on citing](#).

To link to this article DOI: [http://dx.doi.org/10.1007/978-3-030-80439-8\\_13](http://dx.doi.org/10.1007/978-3-030-80439-8_13)

All outputs in CentAUR are protected by Intellectual Property Rights law, including copyright law. Copyright and IPR is retained by the creators or other copyright holders. Terms and conditions for use of this material are defined in the [End User Agreement](#).

[www.reading.ac.uk/centaur](http://www.reading.ac.uk/centaur)

**CentAUR**

Central Archive at the University of Reading

Reading's research outputs online

## Chapter 1

# Impact of granular behaviour of fragmented sea ice on marginal ice zone dynamics

Stefanie Rynders, Yevgeny Aksenov, Daniel L. Feltham, A.J. George Nurser and Gurvan Madec

**Abstract** Sea ice retreat and opening of large, previously ice-covered areas of the Arctic Ocean to wind and ocean waves is leading to large changes in the sea ice state. The Arctic sea ice cover is becoming more fragmented and mobile, with large regions of ice cover projected to evolve into a marginal ice zone (MIZ). Fragmented sea ice has different dynamics, necessitating changes in sea ice model rheology. The objective of this study is to improve sea ice dynamics in models for forecasting and climate projections. We introduce granular behaviour in the ice dynamics and assess the impact on sea ice behaviour. For this purpose we have implemented a seamless rheology for MIZ and pack ice in an idealised sea ice and ocean model. The study compares the effect of the combined rheology with that of the standard elastic-viscous-plastic (EVP) rheology. The main effect of granular behaviour in ice rheology is on internal ice pressure. The jostling of the floes causes divergence of the sea ice cover. Sea ice viscosities are only weakly impacted. In idealised simulations the new sea ice rheology results in widening of the MIZ and a more diffuse ice edge in a stand-alone set-up. Oceanic feedbacks counteract and can undo this effect. The resolution of the simulation modifies the effect of the rheology: a rheology that accounts for granular effects offers better convergence of the solution than the

---

Stefanie Rynders  
National Oceanography Centre, UK, e-mail: s.rynders@noc.ac.uk

Yevgeny Aksenov  
National Oceanography Centre, UK, e-mail: yka@noc.ac.uk

Daniel L. Feltham  
Centre for Polar Observation and Modelling, Department of Meteorology, University of Reading, UK, e-mail: d.l.feltham@reading.ac.uk

A.J. George Nurser  
National Oceanography Centre, UK, e-mail: g.nurser@noc.ac.uk

Gurvan Madec  
Laboratoire d’Océanographie et du Climat: Expérimentations et Approches Numériques (LOCEAN), IPSL, Sorbonne Université, Paris, 75005, France, e-mail: gurvan.madec@locean.upmc.fr

standard EVP. In conclusion, granular sea ice rheology affects the sea ice in the MIZ in some cases, but the importance of the effect in general is not clear.

## 1.1 Motivation

The Arctic sea ice state is changing from typical pack ice conditions to becoming more fragmented and mobile and indeed an increase in marginal ice zone (MIZ, region with ice concentration between 15% and 80%) width is already observed [18]. In the future large regions of the ice cover in summer will evolve into a MIZ according to projections from Aksenov et al. (2017) [1] and the Met Office Hadley Centre (Ed Blockley, personal communication). The MIZ is defined as the region that is influenced by waves, which means its dynamics are different from those of pack ice. In addition to wave effects, sea ice floes in the MIZ can have turbulent motion, defined as random fluctuations in the magnitude and direction of ice motion, which differ from the mean velocity over an area. There are also collisions between sea ice floes. Since sea ice constitutive equations currently used in global ocean-sea ice models are designed for central pack ice, the effect of turbulent motion of the sea ice floes is unaccounted for. The floe motion can influence the stresses in the ice cover as well as impact on the ocean. Turbulent motion of floes can cause increased ocean mixing, potentially influencing stratification and consequently currents. An impact on the mixed layer depth also has implications for biogeochemistry and ecosystems, depending on the season. There is also a growing interest in forecasts for applications: shipping, tourism, fisheries and mineral extraction. These activities are all mainly focussed on the marginal ice zones that are easier to access. The objective of this study is therefore to improve sea ice dynamics in models for forecasting and climate projections, focussing on an improved representation of the MIZ. We examine new sea ice rheologies accounting for the turbulent floe motion as this could be of importance for current and future MIZ conditions.

## 1.2 Marginal ice zone rheology

We introduce granular behaviour in the ice dynamics and assess the impact on the sea ice cover. For this purpose we have implemented a seamless rheology for MIZ and pack ice, that is without switches or other discontinuities, in a coupled sea ice and ocean model. Simulations are performed in an idealised channel model.

Shen first developed a specific rheology for the MIZ specifically, determining the stresses caused by the collisions between floes [15, 16]. This approach is known as collisional rheology. The stresses depend on disk diameter, the restitution coefficient (a measure of how inelastic collisions are) and the magnitude of velocity fluctuations. Stresses are then averaged into a continuum expression of the same form

as a viscous model. Shen's rheology has rarely been used in large scale realistic numerical sea ice simulations, e.g. the Nansen Environmental and Remote Sensing Center (NERSC) have used it in Fram Strait simulations. They used a switch to run collisional rheology in the MIZ alongside EVP rheology for pack ice regions. They encountered frequent problems due to discontinuities in the stresses at the MIZ/pack ice boundary causing numerical instabilities and concluded the approach to be not viable (personal communication). There is also a model for the Sea of Okhotsk from the University of Tokyo which uses a collisional rheology [5]. They combine the collisional rheology of Sagawa (for a semi-lagrangian instead of a continuum model) with viscous-plastic (VP) rheology [14]. The model also contains a switch between the rheologies.

Feltham introduced the 'granular temperature' ( $G_T$ ) of sea ice, an evolving velocity fluctuation magnitude computed from a kinetic energy balance for floes [4]. It allows for a smooth transition between MIZ and pack ice type behaviour. He combined Shen's collisional rheology with VP rheology to create a constitutive law that is suitable for both regions, without a need to predefine a boundary between central pack ice and the marginal ice zone, that avoids numerical issues. Since VP and collisional rheology account for stresses due to different mechanisms, it can be assumed that the internal stress at a point is the sum of both contributions.

**Table 1.1** Combined rheology

	Collisional	EVP
Shear viscosity	$\eta_{COL} = \frac{\gamma(1+e')}{3\pi} \frac{\sqrt{2}G_T^{1/2}}{L_f}$	$\eta_{EVP} = \frac{P}{2\Delta e^2}$
Bulk viscosity	$\zeta_{COL} = \frac{\gamma(1+e')}{\pi} \frac{\sqrt{2}G_T^{1/2}}{L_f}$	$\zeta_{EVP} = \frac{P}{2\Delta}$
Pressure	$P_{COL} = \gamma \frac{\sqrt{2}}{\pi^2} (1+e') \frac{2G_T}{L_f^2}$	$P_{EVP} = g(A)P^*h$
$\gamma = \frac{\rho L_f^2 h}{4} \frac{A^{3/2}}{A_{max}^{1/2} - A^{1/2}}$		
$g(A) = e^{-C(1-A)}$		
$\Delta = \sqrt{(\dot{\epsilon}_{11}^2 + \dot{\epsilon}_{22}^2)(1+e^{-2}) + 4e^{-2}\dot{\epsilon}_{12}^2 + 2\dot{\epsilon}_{11}^2\dot{\epsilon}_{22}^2(1-e^{-2})}$		

Here the collisional rheology is combined with the elastic-viscous-plastic (EVP) rheology [6], with again the different contributions summed. This results in a stress tensor  $\sigma$  as follows:

**Table 1.2** symbols

$G_T$	Granular temperature
$L_f$	Floe size
$e'$	Restitution coefficient
$P^*$	Ice strength
$\rho$	Ice density
$h$	Ice Thickness
$A$	Ice concentration
$A_{max}$	Maximum ice concentration
$C$	ice strength parameter
$e$	Eccentricity of the yield curve
$\dot{\epsilon}$	Strain rate

$$\begin{aligned} \sigma_{ij} = & 2(\eta_{EVP} + \eta_{COL})\epsilon_{ij} + ((\zeta_{EVP} + \zeta_{COL}) - (\eta_{EVP} + \eta_{COL}))\epsilon_{kk}\delta_{ij} \\ & - \frac{1}{2}(P_{EVP} + P_{COL})\delta_{ij}, \end{aligned} \quad (1.1)$$

with  $\epsilon$  the strain rate tensor and  $\delta_{ij}$  the Kronecker delta. The expressions for the bulk viscosity (for isotropic rate dependent deformation), shear viscosity (non-isotropic part of rate dependent deformation) and internal pressure (for plastic deformation) can be found in Table 1.1, with symbols in Table 1.2. The elastic part of EVP rheology exists only for numerical reasons and does not affect the result provided the internal stress calculation converges. We also use a minimum value for the parameter  $\Delta$  to prevent spontaneous viscous creep as in [2]. For the maximum ice concentration in the parameter  $\gamma$  Feltham choose 1, because if floes have different sizes or shapes this value could be reached. For our simulation we follow the approach of Luepkes et al. for their floe size parameterisation and use  $A_*$  instead of  $A_{max}$  to avoid a singularity at 1 [9]:

$$A_* = \frac{1}{1 - (D_{min}/D_{max})^{1/\beta}}, \quad (1.2)$$

with  $D_{min}=8\text{m}$ ,  $D_{max}=300\text{m}$  and  $\beta=0.75$ .  $A_*$  is always slightly higher than 1. The concentration dependency exhibited by the granular temperature ensures that in practice the collisional stress reaches zero at a ‘‘maximum’’ ice concentration (for instance the close packed concentration); the exact point depends on the choice of parameters in the evolution equation [13].

The evolution equation for the granular temperature  $G_T$  is the following:

$$m \frac{\partial}{\partial t} G_T + m \mathbf{u} \cdot \nabla G_T = -\nabla \cdot \mathbf{q} + F - \sigma^T : \nabla \mathbf{u} - \Gamma; \quad (1.3)$$

here  $m$  is the combined mass of the sea ice and the water in between the floes, down to the bottom of the sea ice;  $\mathbf{u}$  is the sea ice velocity and  $\sigma^T$  the transposed stress tensor. The first term in the right hand side of the equation is the divergence of the kinetic energy flux  $\mathbf{q}$ , which redistributes kinetic energy through collisions and ice motion; this is a diffusion term. Then there is an energy source due to

correlation of the turbulent air and ocean drags with the velocity fluctuation ( $F$ ). The final terms are internal stress and energy dissipation  $\Gamma$  ( $\sigma^T : \nabla \mathbf{u}$  is defined as  $\sigma^T : \nabla \mathbf{u} = \sigma_{11} \partial u / \partial x + \sigma_{21} \partial u / \partial y + \sigma_{12} \partial v / \partial x + \sigma_{22} \partial v / \partial y$ ). The granular temperature is treated as an extra tracer in the sea ice model and the energy sources and sinks added separately. The (non-linear) diffusion term is discretised with a simple central difference scheme. This is not a good solution in general as it exhibits checkerboarding, but presently no high time resolution output is used.

### 1.3 Methods

The configuration is an idealised Southern Ocean channel sea ice - ocean model. The ocean model is the hydrostatic general circulation model NEMO (Nucleus for European Modelling of the Ocean)[10]. NEMO is combined with the Los Alamos sea ice model CICE, a dynamic-thermodynamic model with multiple thickness categories [7]. A schematic of the channel model is shown in figure 1.1. The configuration has been constructed starting from an existing ocean-only Southern Ocean channel model, to which the coupling to CICE has been added for this study. The idealised channel has east – west cyclic boundary conditions with land on the northern and southern edges. It extends 2000 km northward from a latitude of 80 degrees south, and has a flat bottom topography.

To be able to distinguish between ice and ocean effects different degrees of coupling are used: an uncoupled channel, a thermodynamically coupled channel and a fully coupled ice – ocean channel. In the uncoupled channel configuration lateral and bottom melting and freezing of the sea ice is disabled. The ocean current is set to zero (in the sea ice model only) and sea surface slope is set to a constant value corresponding to a 3m height difference in the meridional direction over the whole domain. The thermodynamically coupled channel allows all modes of sea ice thermodynamics, but ocean current and sea surface slope are set as in the uncoupled configuration to exclude dynamic interaction with the ocean. A range of configurations is set up at resolutions ranging from 100 km to 12.5 km to examine the convergence of the solution. To limit the resolution dependency of the ocean model solution in all simulations, the lateral diffusion parameters have been adjusted to prevent formation of eddies at high resolution.

All simulations are without daily or seasonal cycles to arrive at a steady state solution. The sea ice is initialised with a 1 m thick ice cover at 100% ice concentration over three quarters of the domain, leaving the northern part ice free; afterwards the ice edge is completely free to move. The sea surface temperature is initialised to a constant value of  $-1^\circ\text{C}$  throughout the water column, chosen to prevent large scale melting or freezing of sea ice right at the start of the simulations. For salinity a realistic depth dependent profile (50°S to 80°S average of PHC climatology with surface set to 30.2 psu [17]) is used to prevent instability of the water column, which

could lead to convection. The atmospheric forcing is a combination of analytical forcing and forcing with realistic latitudinal dependencies. Winds are purely zonal, being westerly at 8.475 m/s over most of the domain and tapering off to zero at the northern and southern edge. Air temperature ranges between  $-5^{\circ}\text{C}$  and  $5^{\circ}\text{C}$ , linearly increasing northward. Short and long wave radiation are also increasing northward with a realistic latitudinal dependency. These forcings are chosen to ensure that ice fully melts towards the northern edge of the domain. Liquid and solid precipitation and humidity are held constant over the domain at realistic mean values. There is no run-off in the channel model.

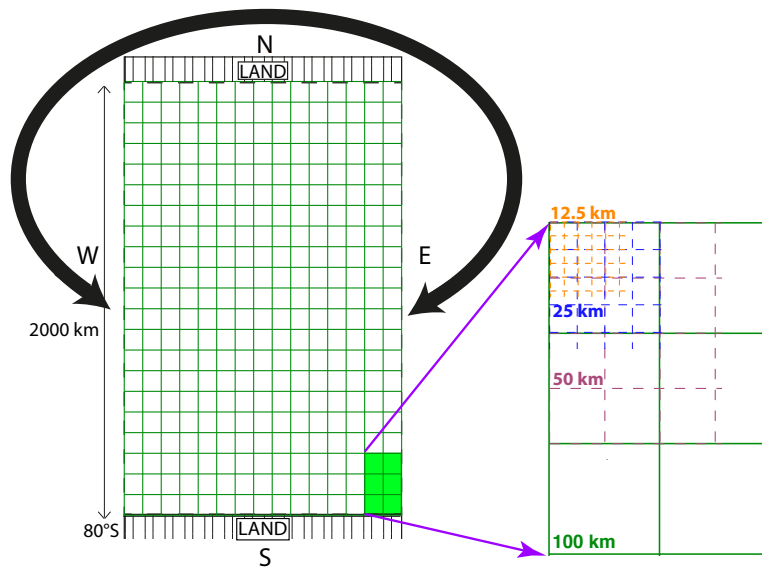


**Fig. 1.1** Schematic of the channel model with the different grid resolutions.

## 1.4 Results

Firstly the effect of the rheology in the uncoupled configuration is examined. Comparing the ice concentration in the EVP simulation to the simulation with the combined EVP and collisional rheology run shows that using the combined rheology causes a wider MIZ (Figure 1.2). This is caused by the jostling of the floes creating a higher internal stress in the MIZ, as is typical for a granular material in the gaslike phase. This causes divergence of the ice cover with the ice edge advancing and becoming more diffuse. To test the convergence of the combined rheology (i.e. the result is

independent of resolution), the model is run at different resolutions and the width of the MIZ with combined rheology is compared to the EVP model. The simulation is run at resolutions of 12.5 km, 25 km, 50 km and 100 km (see Figure 1.3). At 100 km and 50 km resolution both rheologies have equal MIZ widths, saturating at 300 km at 50 km resolution. If the resolution is made finer, the MIZ width with EVP rheology gets progressively smaller. Combined rheology gives a constant MIZ width of 300 km for a resolution of 50 km or higher. This means that the effect of the granular behaviour becomes larger compared to the EVP internal stress. It appears the EVP rheology cannot sustain an MIZ at high resolutions due to a missing source of pressure resulting in too little dispersal.

In the simulations with the thermodynamically coupled channel it can be seen in Figure 1.4 that the simulation with EVP rheology again has a narrow MIZ and the simulation with combined rheology a wider MIZ. In this simulation there is a general melting back of the ice cover. Different to the previous simulations the ice edge is in almost the same position in the EVP and combined rheology. This suggests that the position of the ice edge is dictated by the ocean temperature through ice melting.

Lastly the fully coupled configuration is examined, see figure 1.5. Remarkably there is no change in MIZ width between the two rheologies. The concentration profiles are almost identical except for perhaps a slight decrease in ice concentration in the MIZ in the combined rheology case. This could be caused by granular behaviour if sea ice is being spread out with the ice edge position dictated by the ocean temperature, but it is unclear whether the change is significant.

The different channel model configurations have shown very different results for the uncoupled and thermodynamically coupled simulations than for the fully coupled simulations. The former configurations indeed showed a clear increase in MIZ width with combined rheology, while the latter showed virtually no influence of the granular effects. To investigate this further we examine the total momentum balance in a meridional cross section of the channel for the uncoupled and the fully coupled simulations, both with combined rheology. There is a striking difference in the relative magnitude of the internal stress and the oceanic drag terms in the two simulations. In the uncoupled simulation the internal stress is the third largest term (order  $10^{-2}$  N/m) and the oceanic drag is negligible except close to the ice edge. In the fully coupled simulation on the other hand the internal stress term is small, but the ocean drag term is comparable to the tilt force and only the Coriolis force is clearly larger. The reason for this changed balance can be found in the motion of the sea ice. In the uncoupled simulation the sea ice is moving very slowly. With a static ocean from the point of view of the sea ice this will result in very little ocean drag. In the fully coupled channel model the sea ice moves much faster (northward), and also moves substantially faster than the ocean below, which results in large ocean drag. In the zonal direction atmospheric drag is balanced by oceanic drag, with internal

stress being very small (order  $10^{-3}$  N/m), see figure 1.7a. Given the unimportance of the internal stress in the fully coupled channel model, it can be expected that the combined rheology has no appreciable effect in this setting.

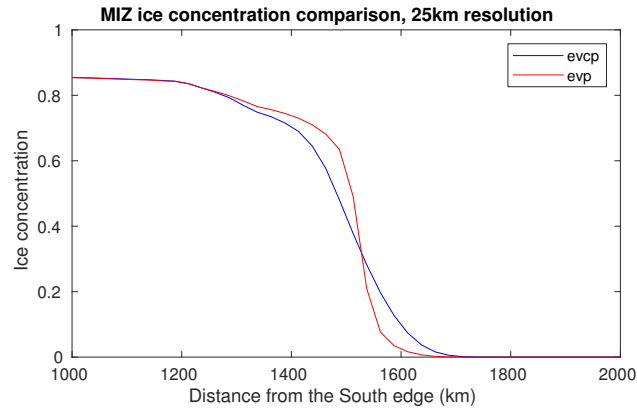


**Fig. 1.2** Dependence of the ice concentration on rheology in the uncoupled channel model. The combined rheology simulation is the blue curve marked evcp; the EVP simulation is the red curve marked evp. Granular behaviour causes a wider MIZ and an advancing ice edge in the combined rheology simulation.

## 1.5 Discussion

In the uncoupled channel model it is evident that there is a substantial increase in MIZ width with the granular rheology compared to the EVP rheology as the resolution of the simulation gets higher. This led to the conclusion that EVP rheology cannot sustain an MIZ through internal mechanisms in the sea ice, whereas the combined rheology can. At sufficiently high resolution it can be expected that the EVP rheology will become unable to sustain a certain MIZ width unless this is being imposed by oceanic influence. This is of concern to the sea ice and ocean modelling community as simulations are performed at ever higher resolutions.

However, in the fully ocean coupled simulation this effect due to the rheology alone is not present. It was found that the lack of sensitivity in the fully coupled simulation is due to the relative unimportance of the internal stress term versus the ocean drag term in the momentum balance (figure 1.6a). When in the future the MIZ forms a major part of the ice cover it is however more likely that low ice concentrations occur in areas of low ocean drag, for instance in places where the ocean current is weak and sea ice velocity low like in the interior Arctic Ocean. This means the effect of the combined rheology is likely to be higher, given the large increase in internal

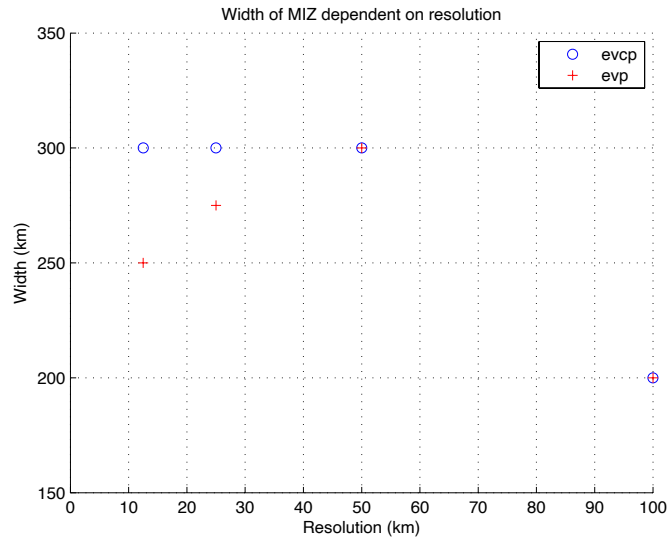


**Fig. 1.3** Dependence of the MIZ width on resolution for EVP and Combined rheology in the uncoupled configuration. For a resolution of 50 km or higher the combined rheology MIZ width is independent of resolution, while with EVP rheology the MIZ narrows as the resolution becomes finer.

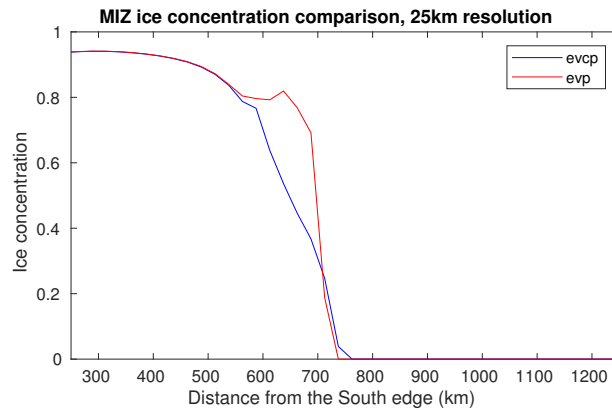


**Fig. 1.4** Dependence of the ice concentration on rheology in the thermodynamically coupled configuration. The combined rheology gives a wider MIZ width than the simulation with EVP rheology.

sea ice stress compared to the EVP rheology in such circumstances. It also means a possible ocean dynamics effect compensating for the low internal stress of sea ice in the MIZ with EVP rheology may be too weak, especially for high resolution simulations. The highest resolution configuration used in the present simulations is 12.5 km. For operational requirements the desired ice edge position uncertainty is

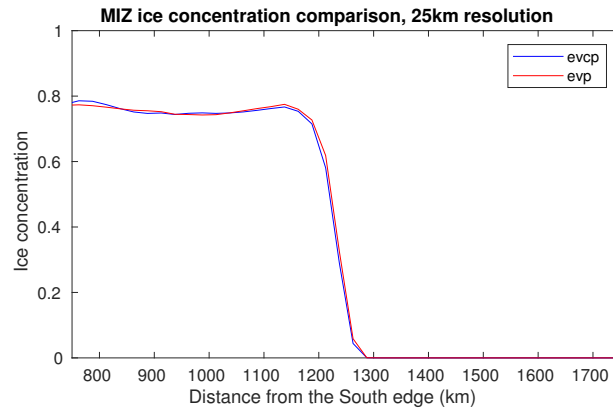


**Fig. 1.5** Dependence of the ice concentration on rheology in the fully coupled configuration.

actually lower (10 km for a 5 day forecast, [3]) than this which means a significant impact even in the fully coupled configuration can not be ruled out and the resolution of the present simulation is in fact too low for firm conclusions.

The granular temperature equation includes energy sources and sinks that are not well known, especially the energy input from turbulent fluctuations in currents and wind. In the present formulation this energy input does not depend on the local ocean velocity, while in reality more turbulence can be expected with faster currents. It is therefore possible that the simulations underestimate the effect of the rheology. The granular temperature calculation used here also does not include a contribution from wave surge. It can be expected that including this effect would result in a higher granular temperature, especially around the ice edge, increasing the impact of the combined rheology and momentum transfer. However, the effectiveness of wave surge in increasing the granular temperature depends on the ratio of the wavelength and the floe size, as well as the ratio of the wave amplitude and the spacing between floes [19].

In the simulations ocean parameters were set so as to suppress possible eddy formation, and the resolution itself was also coarse, to simplify the ice dynamics and analysis of the simulations. Manucharyan et al. examine the impact of eddies in the MIZ in an ice-ocean coupled channel model with VP rheology, but no sea ice thermodynamics [11]. They find that eddies cause a widening of the MIZ, both drawing warmer water into the MIZ and pushing ice outward where it can melt, effectively advancing the ice edge. In the present simulations it was found that the ice edge position is fixed by the ocean surface temperature when full sea ice thermodynamics is allowed. Consequently it can be expected that such a simulation with eddies would result in a more dilute ice edge without advancing it, resulting in a net loss of ice volume. Ice gets exported when it is trapped in cyclonic eddies, so an increase in

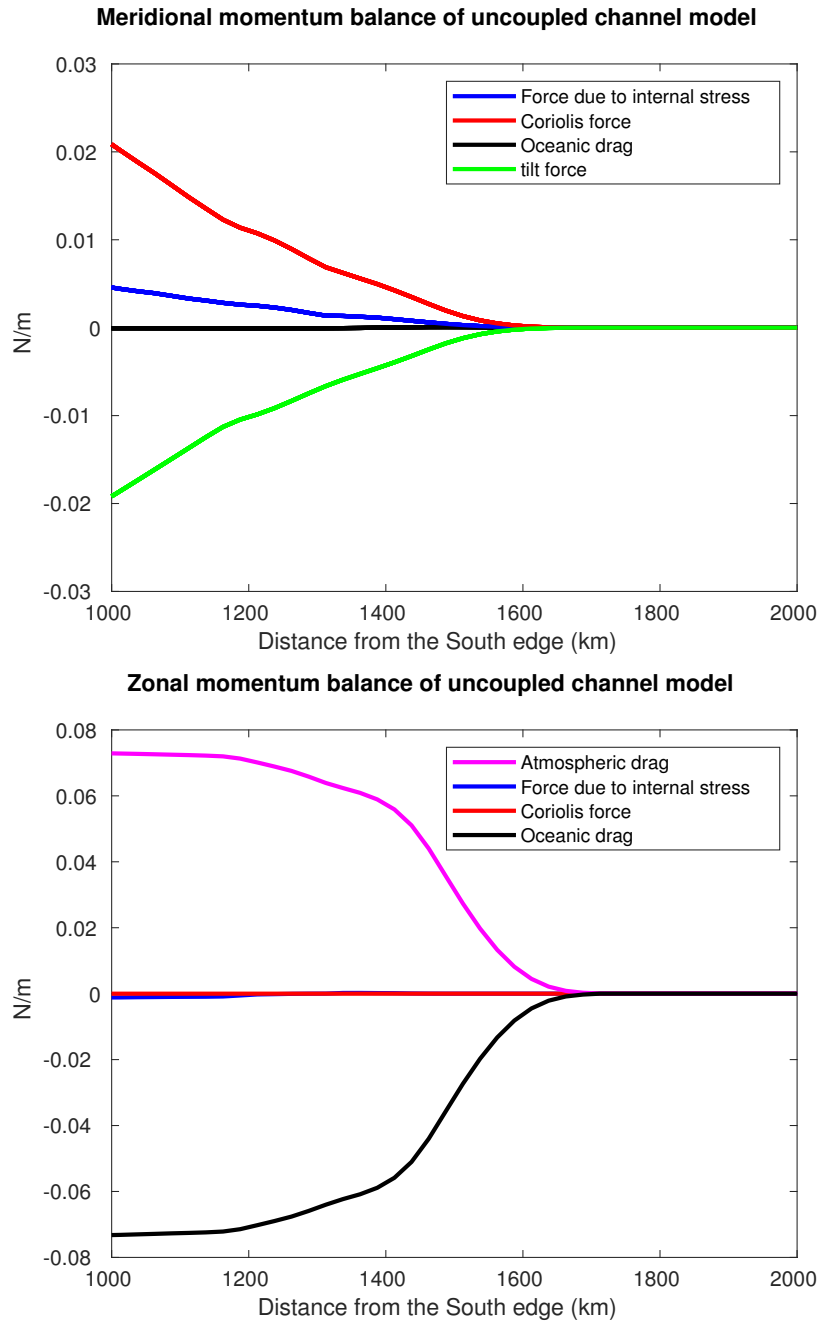


**Fig. 1.6a** Momentum balance of the uncoupled channel model simulation with combined rheology. (a) meridional direction (b) zonal direction.

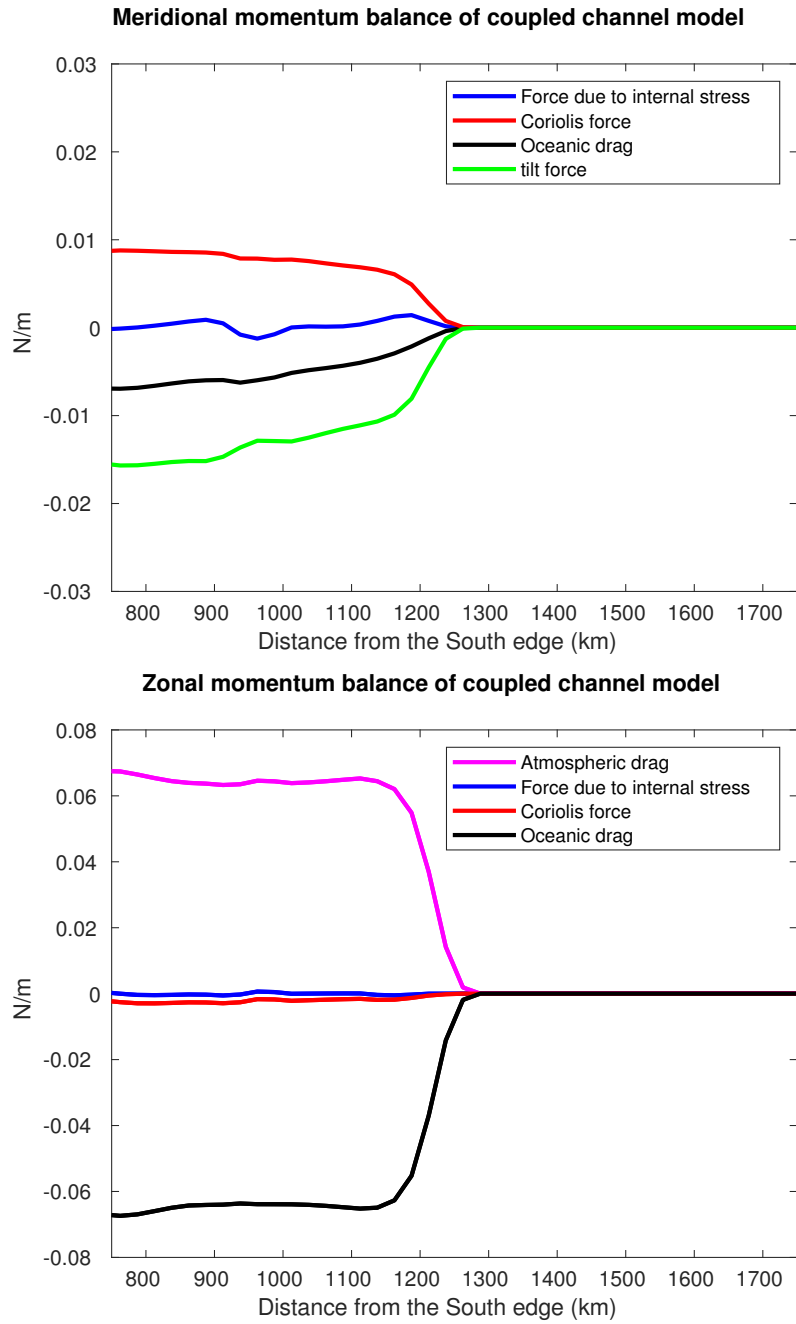


**Fig. 1.7a** Momentum balance of the coupled channel model simulation with combined rheology. (a) meridional direction (b) zonal direction.

internal stress due to granular effects would resist eddy formation more and could delay the process or make the eddy diameter larger. The frontal instabilities may also increase the granular temperature itself. This would be interesting for a future study.

The granular temperature of sea ice floes may be of interest beyond the need for it in collisional rheology. The turbulent motion of ice floes represented by the granular temperature causes extra mixing in the ocean locally, which is not accounted for at the moment. It has also been proposed to use the variance of the ice motion, the granular temperature, to improve oil spill forecasts by estimating the spread in wintertime, when the spill location is inaccessible [12]. Mean term long range forecasts are considered accurate enough, but they are missing part of the small-scale motion which disperses the oil. The granular temperature can be used to calculate the cross section of the oil spill within certain probability limits, assuming a Gaussian distribution of the velocity fluctuations. In the MIZ the jostling of ice floes can cause damage to ships if it causes floes to collide with the flanks of ships. Knowledge of the granular temperature could be used to calculate the loads on the ship and hence be taken into account for risk assessment.

Finally, using the granular temperature to distinguish between MIZ type and pack ice type behaviour is not the only option. Some research has been done on phase transitions in granular materials, which can exhibit gaslike, liquidlike and solidlike behaviour. Ji and Shen suggest an index related to shear rate and concentration for shear flow [8]. Their simulations also highlight that phase transitions are not always sharp, which means an approach with a smoothly changing constitutive law is appropriate. Ji and Shen's results are not a complete solution as sea ice motion can also have a convergent or divergent component. The phase transition of granular materials in general is an unsolved problem and specific research in phase transitions of sea ice as a granular material is lacking. Sea ice is indeed particularly complicated as it is polydisperse, multishaped and the material properties are temperature dependent.

## 1.6 Summary

A combined elastic-viscous-plastic and collisional sea ice rheology has been implemented in a numerical model. Simulations have been carried out in uncoupled, thermodynamically coupled and fully coupled ice-ocean channel models. The new rheology increases MIZ width compared to EVP simulations in the uncoupled channel model. There is no change in width when ocean dynamics are present, due to internal stress being unimportant compared to ocean drag for the momentum balance in this configuration. It was also found that in the case of EVP rheology MIZ width is dependent on resolution for high resolution simulations, whereas the new rheology shows convergence of MIZ width in uncoupled simulations. The conclusion of the study is that MIZ rheology may have an impact when ocean current and drag effects

are weak and floes relatively large, but otherwise rheology does not affect the MIZ width or edge position in divergent conditions.

## 1.7 Acknowledgements

The authors express their gratitude to the International Union for Applied and Theoretical Mechanics for organizing and supporting the Symposium on Physics of Sea Ice in Helsinki in 2019 and providing an excellent forum for discussions and novel ideas. Thanks go to the reviewers for suggestions to extend the discussion and pointing out additional literature sources. This research has been supported by the project ‘Ships and waves reaching Polar Regions (SWARP)’ supported by the European Union’s Seventh Framework Programme (FP7/2007-2013) under grant agreement No 607476 and also by the UK project “Towards a marginal Arctic sea ice cover” (NE/R000654/1). This project has also received funding from the European Union’s Horizon 2020 research and innovation programme under grant agreement No 821926 (project IMMERSE – Improving Models for Marine EnviRonment SERVICES). This paper, reflects only the authors’ view; the European Commission and their executive agency are not responsible for any use that may be made of the information the work contains.

## References

- [1] Aksenov, Y.; Popova, E.; Yool, A.; Nurser, A. J. G; Bertino, L.; Williams, T. D., and Bergh, J. On the future navigability of the Arctic sea routes: High-resolution projections of the Arctic Ocean and Sea Ice decline. *Mar. Policy*, 75:300–317, January 2017.
- [2] Bouillon, S.; Fichet, T.; Legat, V., and Madec, G. The elastic-viscous-plastic method revisited. *Ocean Model.*, 71:2–12, November 2013. doi: 10.1016/j.ocemod.2013.05.013.
- [3] De Silva, L. W. A. and Yamaguchi, H. Grid size dependency of short-term sea ice forecast and its evaluation during extreme Arctic cyclone in August 2016. *Polar Science*, 21:204 – 211, 2019. ISSN 1873-9652. doi: 10.1016/j.polar.2019.08.001. ISAR-5/ Fifth International Symposium on Arctic Research.
- [4] Feltham, D.L. Granular flow in the marginal ice zone. *Phil. Trans. R. Soc. A*, 363:1677–1700, July 2005. doi: 10.1098/rsta.2005.1601.
- [5] Fujisaki, A.; Yamaguchi, H., and Mitsudera, H. Numerical experiments of air–ice drag coefficient and its impact on ice–ocean coupled system in the Sea of Okhotsk. *Ocean Dynamics*, 60(2):377–394, Apr 2010. ISSN 1616-7228. doi: 10.1007/s10236-010-0265-7.

- [6] Hunke, E. C. and Dukowicz, J. K. An Elastic–Viscous–Plastic Model for Sea Ice Dynamics. *J. Phys. Oceanogr.*, 1997.
- [7] Hunke, E.C.; Lipscomb, W.H.; Turner, A.K.; Jeffery, N., and Elliott, S. *CICE: the Los Alamos Sea Ice Model Documentation and Software User’s Manual Version 5.0 LA-CC-06-012*. Los Alamos National Laboratory, Los Alamos NM 87545, December 2013.
- [8] Ji, S. and Shen, H. H. Internal parameters and regime map for soft polydispersed granular materials. *Journal of Rheology*, 52(1):87–103, 2008. doi: 10.1122/1.2807441.
- [9] Luepkes, C.; Gryanik, V. M.; Hartmann, J., and Andreas, E. L. A parametrization, based on sea ice morphology, of the neutral atmospheric drag coefficients for weather prediction and climate models. *J. Geophys. Res.*, 117(D13): D13112, July 2012. doi: 10.1029/2012JD017630.
- [10] Madec, G. *NEMO ocean engine (Draft edition r5171)*. Note du Pole de modelisation, Institut Pierre-Simon Laplace (IPSL), France, no 27 issn no 1288-1619 edition, 2014.
- [11] Manucharyan, G. E. and Thompson, A. F. Submesoscale Sea Ice–Ocean Interactions in Marginal Ice Zones. *Journal of Geophysical Research: Oceans*, 122(12):9455–9475, 2017. doi: 10.1002/2017JC012895.
- [12] Rampal, P.; Bouillon, S.; Bergh, J., and Ólason, E. Arctic sea-ice diffusion from observed and simulated Lagrangian trajectories. *Cryosphere*, 10(4):1513–1527, July 2016. doi: 10.5194/tc-10-1513-2016.
- [13] Rynders, S. *Impact of surface waves on sea ice and ocean in the polar regions*. PhD thesis, University of Southampton, Ocean and Earth Sciences, 2017.
- [14] Sagawa, Genki and Yamaguchi, Hajime. A Semi-Lagrangian Sea Ice Model for High Resolution Simulation. In *Proceedings of the Sixteenth (2006) International Offshore and Polar Engineering Conference*, pages 584–590. The International Society of Offshore and Polar Engineers, 2006.
- [15] Shen, H.H; Hibler, W.B., and Lepparanta, M. On applying granular flow theory to a deforming broken ice field. *Acta Mech.*, 63(1-4):143–160, 1986.
- [16] Shen, H.H; Hibler, W.B., and Lepparanta, M. The role of floe collisions in sea ice rheology. *J. Geophys. Res.*, 92(C7):7085–7096, June 1987. doi: 10.1029/JC092iC07p07085.
- [17] Steele, M.; Morley, R., and Ermold, W. PHC: A Global Ocean Hydrography with a High-Quality Arctic Ocean. *Journal of Climate*, 14(9):2079–2087, 2001. doi: 10.1175/1520-0442(2001)014<2079:PAGOHW>2.0.CO;2.
- [18] Strong, C. and Rigor, I. G. Arctic marginal ice zone trending wider in summer and narrower in winter. *Geophys. Res. Lett.*, 40(18):4864–4868, September 2013. doi: 10.1002/grl.50928.
- [19] Yiew, L. J.; Bennetts, L. G.; Meylan, M. H.; Thomas, G. A., and French, B. J. Wave-induced collisions of thin floating disks. *Physics of Fluids*, 29(12): 127102, 2017. doi: 10.1063/1.5003310.